INTERNATIONAL JOURNAL OF INTEGRATED ENGINEERING
ISSN: 2229-838X e-ISSN: 2600-7916

IJIE

Vol. 16 No. 5 (2024) 56-70
https://publisher.uthm.edu.my/ojs/index.php/ijie

Effect of Nano A-Mno$_2$ Addition on Thermal Decomposition and Compressive Properties of Epoxy

Md. Zakir Hussain[1], Pranjal Sarmah[2]*

[1] *Lecturer, Department of Mechanical Engineering, DSEU Wazirpur Campus 1, New Delhi, 110052, INDIA*
[2] *Assistant Professor, Department of Mechanical Engineering, Dibrugarh University, Dibrugarh, 786004, INDIA*

*Corresponding Author: pksnit07@gmail.com
DOI: https://doi.org/10.30880/ijie.2024.16.05.006

Article Info

Received: 12 January 2024
Accepted: 23 May 2024
Available online: 1 August 2024

Keywords

Nanocomposites, manganese dioxide, epoxy, thermal analysis, compression

Abstract

The ability of a nanocomposite material to withstand high temperatures and maintain strength is crucial for the design of products and processes. This research examined the thermal decomposition and compressive properties of α-MnO_2/epoxy polymer nanocomposites. The samples were created using a simple, inexpensive solution technique. The scanning electron microscope, X-ray diffraction, and energy-dispersive X-ray analysis indicated the formation of α-MnO_2 nanosheets. The thermal analysis revealed that the addition of α-MnO_2 increased the glass transition temperature of the epoxy. Thermogravimetric analysis showed that the residue was left at 550°C for a sample of pure epoxy with a loading of 0.1 wt.%. 0.2 wt.%, 0.3 wt.%, and 0.5 wt.% of α-MnO_2 were 9.55%, 11.05%, 16.78%, 17.37%, and 21.20%, respectively. As a result, the nanocomposites were more thermally stable than pure epoxy. The compressive characteristics were tested using a universal testing machine. Compression test results showed that the addition of α-MnO_2 decreased the compressive properties of the epoxy matrix. However, the brittleness of nanocomposites increased. Images captured at the microscopic level showed that the sample cracked and fractured during testing. The reduced compressive property values was associated with reduced α-MnO_2 dispersion in the epoxy, the shape of α-MnO_2 nanosheets, and the generation of air voids during the synthesis process. As a result, the α-MnO_2 nanosheets reduce the compressive properties of the nanocomposites by acting as stress enhancers. The nanocomposite can be used as a thermal heat-resistant material.

1. Introduction

The ability of a polymeric material to withstand heat and maintain its properties, such as strength or elasticity, at elevated temperatures is referred to as thermal stability. The composite's exceptional compressive strength may be attributed to its excellent thermal stability [1]. Most engineering materials are classified according to how well they withstand mechanical stress, which applies to all materials. They are measured by how long a material can sustain forces before failing. The properties of engineering materials are improved by adding nanomaterials into the matrix. Nanomaterials are manufactured and used when they have at least one nanometer-sized phase dimension, which is intermediate between the structural features of atoms and bulk materials [2]. They can combine two materials such that the resulting material is of higher quality than the components that comprise it.

This is an open access article under the CC BY-NC-SA 4.0 license.

Because of their high aspect ratio, nanomaterials often provide excellent reinforcing characteristics [3]. The size scales of the component phases of a nanocomposite, as well as the degree of phase mixing, have a substantial influence on the material's properties. The type of components used and the preparation technique can produce significant changes in composite quality [4]. Inadequately distributed filler aggregates behave as defect sites, thereby restricting the mechanical performance; such agglomerates can have a detrimental influence on composite characteristics.

Continuous polymeric material phase and one or more discontinuous dispersion phases, such as quantum dots, carbon nanotubes, nanorods, nanowires, nanofibers, layered materials, or spherical particles, constitute polymer nanocomposites [5]. Polymers are frequently utilized as matrix materials due to their dimensional stability, lightweight, durability, low cost, simplicity of manufacturing, and corrosion resistance. However, the materials' insufficient mechanical, heat resistance, wear, electrical, and gas barrier characteristics restrict their use in scientific disciplines when compared to metal and ceramic-based nanocomposites. The creation of an irreversible 3-D cross-linked structure after curing makes thermosetting polymers very resistant to altering shape when heated [5–6]. When compared to thermoplastic materials, this kind of polymer exhibits the behavior of brittle materials. The composition of thermosetting polymers makes up about 15-20% of the total quantity of plastic used worldwide [6]. The low-value utilization of thermosetting polymers is brought on by their brittle character as compared to thermoplastic materials.

Epoxy resin is a common substance used in the production of high-performance nanocomposites. Because of their geometrical consistency, simplicity of synthesis at room temperature, strong adhesive capability, excellent mechanical capabilities, resistance to corrosion, and temperature resistance, resin-based nanocomposite materials are commonly used for developing innovative material applications [7]. Adhesives in electronic equipment, laminates, surface coatings, car components, energy, water pipelines, food packaging, sports, aircraft parts, and naval systems are the most common uses for epoxies.

Due to its affordability, environmental friendliness, and exceptional capacitive performance in aqueous electrolytes, manganese dioxide (MnO_2) is recognized as a suitable electrode material [8-12]. MnO_2 can have several structural and electrical forms, including metallic, semiconductor, and insulator. Balguri et al. investigated the reinforcing effects of nanoflower and nanowires-type MnO_2 using tensile, flexural, and impact tests. They demonstrated that MnO_2 nanostructures considerably boosted the mechanical characteristics of epoxy [13]. Hussain et al. studied the tribological characteristics of α-MnO_2-epoxy nanocomposites and reported that the wear resistance and friction behavior of the α-MnO_2-epoxy nanocomposites increased with the addition of α-MnO_2 to the epoxy [14]. The researchers did not explore the mechanical properties of sheet-type α-MnO2/epoxy nanocomposite. Qian et al. noticed that adding α-MnO_2 to multi-walled carbon nanotubes (MWCNT)-epoxy nanocomposites increased their fire safety [15]. According to Zhou et al., the toughness, elongation at break, tensile strength, and flexural strength of epoxy were all greatly improved by trace functional graphite oxide addition [16]. Che Nasir et al. showed that the homogeneous dispersion, size, and shape of nanoparticles had a substantial impact on the outcome characteristics of the epoxy matrix [17]. The functionalized hexagonal boron nitride nanoflakes was successful in increasing the toughness, elastic modulus, and tensile strength of epoxy [18], by establishing a high affinity between the fillers and the matrix. When compared to clean epoxy, epoxy nanocomposites containing 2 weight percent (wt.%) alumina and 0.5 wt.% graphene nanoplatelets showed a significant improvement in flexural strength and modulus [19]. Due to better interfacial contact between the filler and the base material, Wu et al. found that adding graphene oxide increased the aramid fiber/flexural epoxy's strength and modulus compared to pure epoxy resin [20]. Yusuf et al. employed the Taguchi approach to increase the tensile and flexural strengths of composites made using epoxy resin reinforced with sponge gourd, coir, and jute fibers [21]. The ANOVA findings revealed that the wt.% ratio of resin and hardener, as well as the wt.% ratio of sponge gourd and jute, affected both tensile and flexural strength. According to Reddy et al., the inclusion of fly ash increased the tensile and flexural properties of glass fiber epoxy composites [22]. Hamim et al. studied the combined influence of moisture and increased temperature on the mechanical characteristics of clay/epoxy nanocomposites [23]. According to the researchers, hygrothermal aging reduced fracture toughness, flexural strength, and modulus in both the neat polymer and the clay/polymer nanocomposite. Due to the homogeneous dispersion of reduced graphene oxide in the epoxy, Khan et al. noticed that mechanical parameters including impact strength, hardness, tensile strength, and Young's modulus increased with a rise in reduced graphene oxide up to 0.3 wt.% loading [24]. On the other hand, the thermal characteristics did not greatly improve. Norhakim et al. observed that the mechanical characteristics of epoxy nanocomposites were greatly enhanced through the inclusion of graphene oxide [25]. Compared to the neat epoxy sample, the flexural strength of the composite sample containing 0.3 wt.% graphene oxide was improved by roughly 50%. The impact strength of the composite was only marginally enhanced by the addition of 0.1 wt.% graphene oxide. Mohammed et al. observed that microhardness, impact energy, and flexural strength were all increased by uniformly dispersing MWCNTs and Al2O3 nanoparticles. However, the tensile strength was dramatically decreased by the dispersion of the aforementioned nanofillers [26]. The creation and mechanical characteristics of epoxy polymer composite materials created with hard ceramic fillers like Al_2O_3, SiO_2, MgO, and TiO_2 were examined by Ergün et al. [27]. For

flexural strength, modulus, and hardness, their research showed that additions with better distribution produced superior results; nevertheless, for impact toughness, the additive's grain size had also become important. Vila et al. demonstrated that the emergence of graphene pileups in the epoxy matrix and their dispersion around the carbon fibers had a substantial influence on the bending strength [28]. The mechanical characteristics of carbon fiber (CF)/epoxy composites containing various kinds of MWCNT were studied by Siegfried et al. [29]. It was observed that the MWCNT served more as a crack initiator than reinforcement during compression and impact testing. They concluded that the mechanical features of the specimens were impacted by the MWCNT dispersion state. MWCNT/epoxy nanocomposites' mechanical characteristics were studied by Singh et al. with various MWCNT fillers [30]. The research found that the better dispersion of the MWCNT filler in the epoxy matrix enhanced the mechanical characteristics of the nanocomposites, such as tensile strength, compressive strength, and elastic modulus. Srivastava and Singh investigated the elastic modulus of MWCNT/epoxy resin [31]. The results showed that increasing the proportion of MWCNTs reinforcement boosted the nanocomposites' mechanical features. Giovannelli et al. developed MWCNT/epoxy nanocomposites through mechanical mixing [32]. The results of the tensile and compressive tests revealed a rise in Young's modulus and compressive property in comparison to the pristine resin. The MWCNT's potential as a filler for epoxy-based nanocomposites was eventually confirmed by the researchers. Finally, it is crucial to understand that research on nanocomposite materials has applications across a broad spectrum, including those in electronics and computers, data storage, communications, aircraft, sports goods, medicine, energy, the environment, transportation, and national security [33].

Many researchers found that the wear resistance of sheet-type α-MnO_2/epoxy nanocomposite, tensile strength, flexural strength, and impact strength of nanoflower and nanowire-type α-MnO_2/epoxy nanocomposite increased with the addition of α-MnO_2. However, the thermal and mechanical properties of sheet type α-MnO_2/epoxy nanocomposite have not been fully explored to date. Therefore, the ongoing research focuses on the effect of α-MnO_2 nanosheets on the thermal decomposition, and compressive characteristics of the epoxy matrix.

2. Materials and Techniques

2.1 Materials

Chemicals such as tetramethylammonium hydroxide, H_2O_2, and $MnCl_2$ were used to synthesize α-MnO_2. The chemicals were obtained from North East Chemicals, Assam. The polymeric resin utilized in this study was an epoxy resin called LAPOX L-12. The hardener K-6 was utilized to cure the epoxy resin as a curing specialist. The resin and hardener were acquired from M/S Atul Chemicals, Gujarat.

2.2 Fabrication of α-MnO_2 Nanosheets

We synthesized α-MnO_2 nanopowder in this study using a simple solution technique that Wang et al. described [15, 34-35]. The usual procedure was to add 40 ml of 0.3 $MnCl_2$ (aqueous), 24 ml of 1.0 M tetramethylammonium hydroxide, 4 ml of 30 wt.% H_2O_2, and 30 ml of de-ionized water to the mixture and stir it for 15 s. A magnetic stirrer (make: IKA, Germany) was then used to agitate the liquid continuously for 12 hours at room temperature. The dark yield eventually became evident due to constant stirring. The completed product was repeatedly rinsed in de-ionized water and acetone to eliminate any unwanted ions that may have remained before being dried in a hot air heater for 48 hr at 60°C.

2.3 Fabrication of Epoxy and Nanocomposites

2.3.1 Preparation of Epoxy

The fabrication approach for pure epoxy samples is solution mixing [14]. First, a glass rod was used to gently and gradually pour the epoxy resin into the beaker. The epoxy resin's surface-level bubbles were eliminated using the bell-pin. Epoxy resin was first ultrasonically cleaned in a Buehler ultrasonic cleaning bath for 10 min. The temperature of the mix was consistently maintained at an ambient temperature, or 24°C, to prevent resin deterioration. After ultrasonication, LAPOX K-6, a hardener, was introduced to the slurry in a wt. ratio of 1:10 with epoxy resin. The resultant mixture was then stirred for a further 5 min using a magnetic stirrer, followed by another 5 min of ultrasonically cleaning. The solution was placed into the mold. The leftover bubbles that were in the mold could be removed with a bell-pin. The mold was dried at room temperature. Figure 1 (a) depicts the prepared epoxy specimens for the compression test.

2.3.2 Preparation of α-MnO_2/Epoxy Nanocomposites

The processing method employed to distribute α-MnO_2 in epoxy resin was the solution method [14]. The 0.5 wt.% of α-MnO_2 powder was initially added to the 250 ml beaker. The beaker was then gently filled with the resin using a glass rod to avoid generating too many bubbles as it was being poured. α-MnO_2 powder and epoxy resin were stirred for 30 min to mix the powder and resin. In an ultrasonic cleaning bath, the slurry was pre-sonicated for 3 hr (brand: Buehler). Using a tip-sonicator, the pre-sonicated mix was exposed to a 30 min tip sonication (sonics, 750 Watts, 20 kHz) procedure. The temperature of the mix was continually kept below 400C by employing an ice water bath to minimize resin deterioration. The pulse on and off timings were maintained at 10 s and 60 s, respectively, throughout the tip-sonication process. The pulse-off time is kept at a larger magnitude to keep the mixture's temperature from exceeding 40°C. Then, with the aid of a magnetic stirrer, hardener K-6 and epoxy resin were mixed in a wt. ratio of 1:10 each. After stirring the final mixture for 5 min, the bubbles that remained were eliminated using an ultrasonic cleaning bath. The mixture was then transferred to the mold using a glass rod, where it was permitted to dry for 48 hr at room temperature. Figure 1(b) displays the prepared 0.5 wt.% α-MnO_2/epoxy nanocomposite samples for compression test. We also fabricated additional α-MnO_2/epoxy nanocomposite specimens similarly.

(a) **(b)**

Fig. 1 *The prepared compressive test samples (a) epoxy; (b) 0.5 wt.% loading of α-MnO_2*

2.4 Thermal Characterization

To assess the samples' thermal stability, a simultaneous thermal analyzer (make: Perkin Elmer, model: STA 6000/8000) was used to conduct a thermo-gravimetric (TG) examination of the samples. In the present investigation, a 10 mg sample was analyzed under isothermal circumstances at a flow rate of 19.8 ml/min in an argon (Ar) environment, scanning temperatures between 300°C and 550°C.

2.5 Compression Test

The ASTM standard D-695 was pursued by conducting the compressive test. At 18°C, the samples were put in their places on the Instron Dynamic Universal testing apparatus. (brand: Instron; UK). Using the device's Blue Hill software, real-time graphs can be recorded. The machine has a 10 kN capacity. The load cell has a capacity of 100 kN, and the longest crosshead travel distance is 1505 mm. Linear, biaxial, and temperature-resistant describe the extensometer. The specimen is set on the machine's flat surface for testing, and then it is compressed until it breaks. The compressive properties of each sample were determined by averaging the results of three experiments.

3. Results and Discussion

3.1 X-ray Diffraction Pattern of α-MnO_2/Epoxy Nanocomposites

A non-destructive analytical method known as X-ray diffraction (XRD) can reveal information about a material's chemical composition, physical properties, and crystallographic structure. To address all issues about the crystal structure of solids, XRD is an extremely important experimental technique.

The collection of experimental data on diffraction was recorded using an X-ray diffractometer (model: Rigaku ULTIMA IV) using Cu-Kα radiation operating at a voltage of 30 kV and a tube current of 15 mA. Figure 2 demonstrates the XRD results for 0.5 wt.% α-MnO2. The lattice constants of the tetragonal α-MnO2 single crystal structure for the space group I4/m (87) are a = b = 9.815 Å and c = 2.847 Å and can index the 0.5 wt.% α-MnO_2

Int. Journal of Integrated Engineering Vol. 16 No. 5 (2024) p. 56-70

XRD diffraction pattern. α-MnO_2 diffraction peaks were obtained at 2θ values of 12.14°, 17.9°, 28.74°, 37.44°, 41.68°, 49.52°, 55.82°, 59.86°, 65.34°, and 69.16°, and the corresponding lattice planes were planes (110), (200), (310), (211), (301), (411), (600), (521), (002), and (541) respectively. The overall diffraction peak positions found for α-MnO_2 were consistent with those found by others [36–40]. The existence of single-crystal α-MnO2 nanosheets was demonstrated. The sample 2θ value of 37.47° is where the largest peak is located.

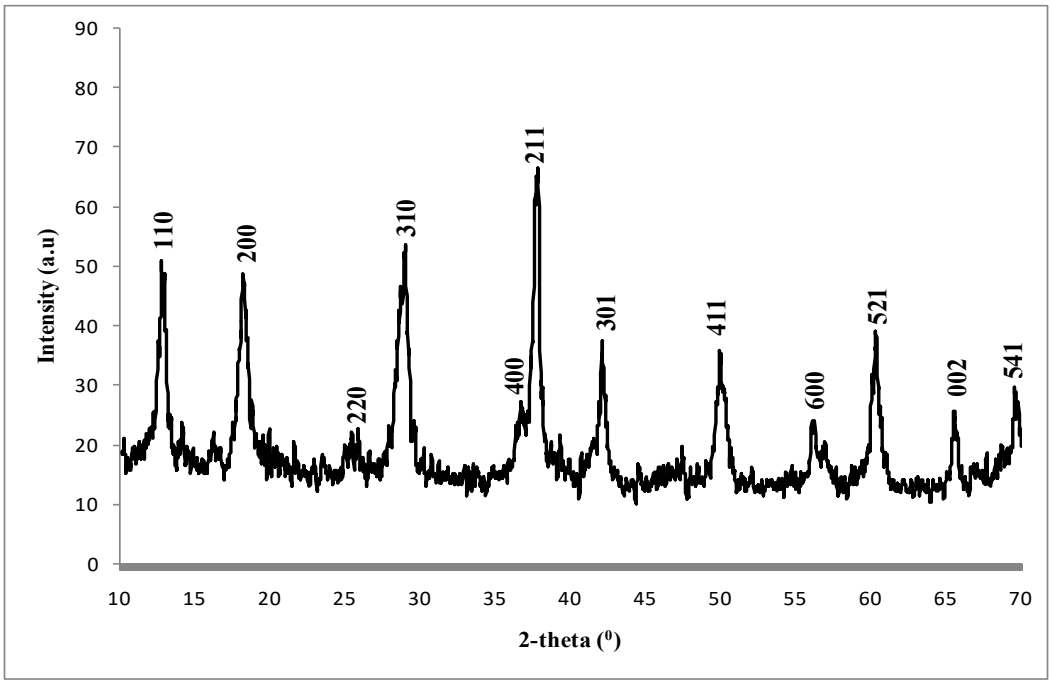

Fig. 2 *XRD pattern of α-MnO_2*

3.2 Surface Morphology of Samples

This high-resolution field emission scanning microscope's (HRFESEM's) main function is to look at the nanocomposites' microstructure. HRFESEM (make: Zeiss) was used to examine the surface morphology of α-MnO_2/epoxy nanocomposites. HRFESEM surface morphology pictures of various wt.% of α-MnO_2/epoxy nanocomposites are shown in Figure 3. Figure 3(a) demonstrates that the epoxy's surface is smooth. Figures 3(b)–(d) demonstrate that the exterior of the epoxy includes bundles of α-MnO_2 nano-sheets with sizes in the nanometer range ξ 25 nm) [34]. The shape of α-MnO_2 has a plate-like structure. Comparatively, to other nanocomposites, the sample containing 0.5 wt.% of α-MnO_2 loading in the epoxy matrix exhibits homogeneous α-MnO_2 nanosheet distribution.

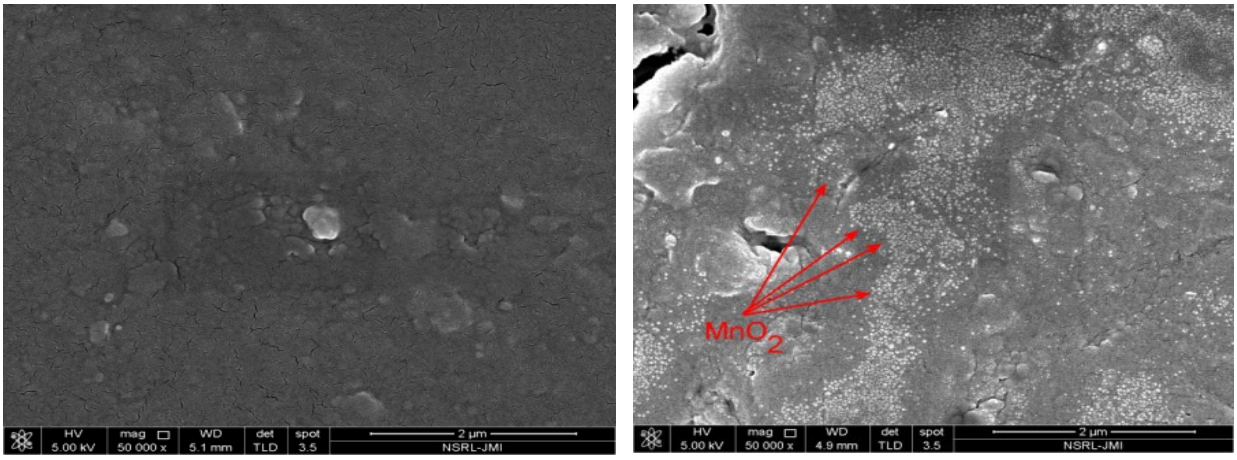

(a) **(b)**

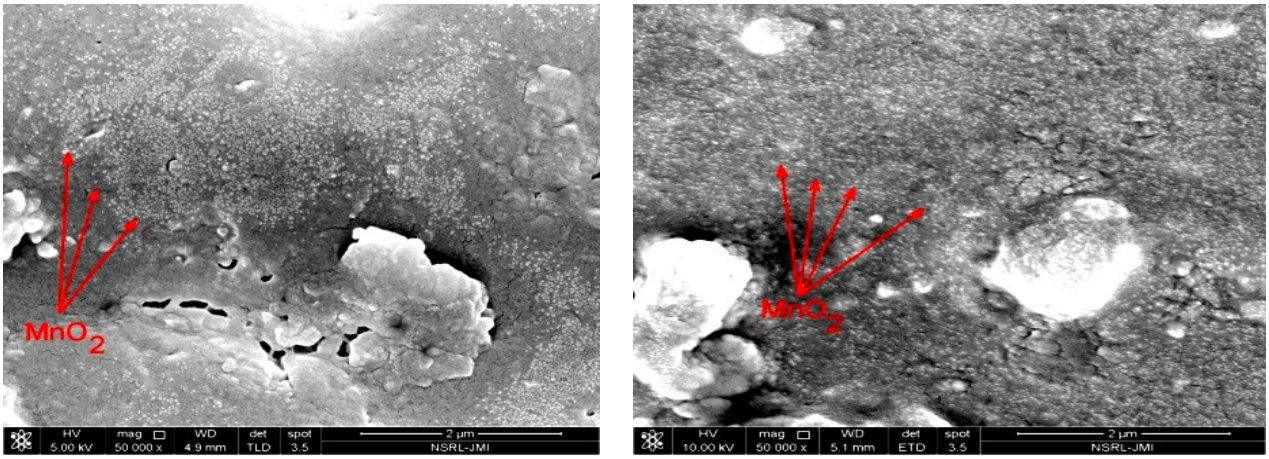

(c) **(d)**

Fig. 3 *Surface morphology of neat samples (a) epoxy; (b) 0.1 wt.%; (c) 0.3 wt.%; (d) 0.5 wt.% loading of α-MnO_2*

3.3 Chemical Elements of Nanocomposite

To ascertain the chemical components of composite materials, energy dispersive X-ray analysis (EDX), an X-ray method, is performed. The energy-dispersive spectrum of the α-MnO_2 epoxy nanocomposite is displayed in Figure 4, along with an inset that shows where it was collected. The manganese (Mn) and oxygen (O) chemical components are visible on the surface of the α-MnO_2/epoxy nanocomposite. The elemental study, therefore, validates the production of α-MnO_2 nano-sheets [41].

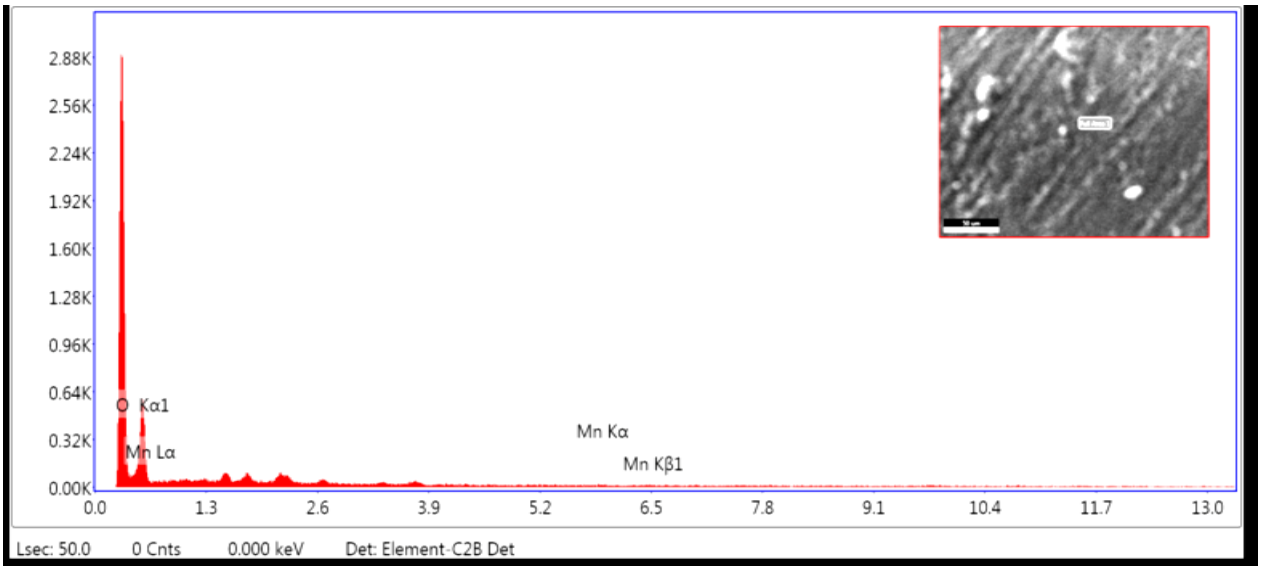

Fig. 4 *EDX spectrum of 0.3 wt.% α-MnO_2 of loading*

3.4 Density of Epoxy and Nanocomposites

Archimedes' principle may be used to determine the epoxy and α-MnO_2/epoxy nanocomposite's mass density. The samples were initially weighed in the air. The volume displacement is shown by the volume change brought on by completely immersing the sample. Next, we determined the epoxy and nanocomposite samples' mass density using Archimedes' method. Distilled water has a density of 0.997 g/cm^3 at 25°C. Three trials were utilized to obtain the average density. The densities of the epoxy and α-MnO_2/epoxy nanocomposite samples are displayed in Table 1. Epoxy has a density of 1.1825 g/cm^3 on average. The sample loadings of 0.1 wt.% α-MnO_2, 0.2 wt.% α-MnO_2, 0.3 wt.% α-MnO_2, and 0.5 wt.% α-MnO_2 had densities of 1.196 g/cm^3, 1.214 g/cm^3, 1.224 g/cm^3, and 1.236 g/cm^3, respectively. The density fluctuation shows that the addition of high-density α-MnO_2 causes an increase in density with wt.% loading of α-MnO_2 in the epoxy [38].

Int. Journal of Integrated Engineering Vol. 16 No. 5 (2024) p. 56-70

Table 1 *Density of specimens*

Sl no.	Specimens	Density (g/cm^3)
1	0.0 wt.% loading of α-MnO_2/epoxy nanocomposite	1.1825
2	0.1 wt.% loading of α- MnO_2/epoxy nanocomposite	1.196
3	0.2 wt.% loading of α- MnO_2/epoxy nanocomposite	1.214
4	0.3 wt.% loading of α- MnO_2/epoxy nanocomposite	1.224
5	0.5 wt.% loading of α- MnO_2/epoxy nanocomposite	1.236

3.5 Thermal Analysis

3.5.1 Glass Transition Temperature of Samples

Figure 5 shows the differential scanning calorimetric curves for the specimens. The graph shows that the glass transition temperatures for epoxy and nanocomposites with 0.1 wt.% α-MnO_2, 0.2 wt.% α-MnO_2, 0.3 wt.% α-MnO_2, and 0.5 wt.% α-MnO_2 loadings are, respectively, 70.30°C, 73.20°C, 75.40°C, 77.30°C, and 79.80°C. As a result, introducing α-MnO_2 improved the epoxy's glass transition temperature. The inclusion of α-MnO_2 decreased the heat carried through the nanocomposites. The formation of dispersed α-MnO_2 within the epoxy and the arrangement of a strong cross-linked network structure can contribute to the elevated glass transition temperature of the nanocomposites [14].

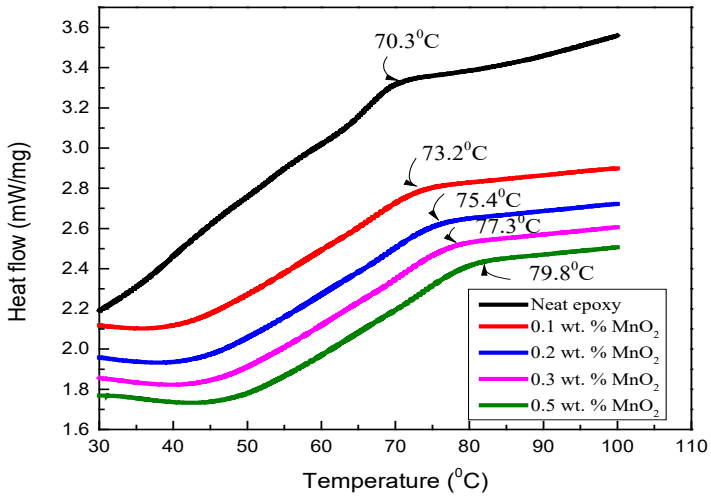

Fig. 5 *The glass transition temperature of sample*

3.5.2 Thermo Gravimetric Analysis

The Thermo gravimetric analysis (TGA) curves shown in Figure 6 depict the onset of degradation temperatures of epoxy, 0.1 wt.% α-MnO_2, 0.2 wt.% α-MnO_2, 0.3 wt.% α-MnO_2, and 0.5 wt.% α-MnO_2 loading in the epoxy are 361.67°C, 360.97°C, 363.20°C, 362.18°C, and 357.67°C, and the corresponding mass losses are 14.26%, 13.18%, 9.84%, 7.84%, and 5.72%, respectively. The final degradation temperatures of all the samples are 550°C. Table 2 shows the TGA data of epoxy composites at different temperatures. The weight loss of samples of around~ 2-3% was observed at 100°C, which may be due to the release of moisture corresponding to the absorption of heat. Between the temperatures of 100°C-550°C, the weight loss of all samples is attributed to the removal of a small content of water and degradation of the epoxy matrix. MnO_2 is an inorganic compound and does not degrade below 500°C [42]. The weight loss above 500°C is attributed to the reduction of Mn^{4+} species and the formation of Mn_2O_3 [42], and the decomposition of the polymer. Figure 6 shows that the nanocomposite samples had a comparable degradation path, indicating that the presence of α-MnO_2 did not appreciably modify the epoxy matrix`s degradation mechanism [43]. Figure 6 shows the main degradation peak in all the samples that occurred between 325°C and 475°C, accompanied by the corresponding weight loss of 70%–75%. Table 3 shows the TGA data of epoxy and nanocomposites at different % of mass loss. The sample with a 0.5 wt.% loading exhibits a smaller weight percent loss than the other samples. The epoxy sample shows a 5% wt. loss at 175.31°C. Similarly,

the 5% wt. loss for the samples containing 0.1 wt.% α-MnO_2, 0.2 wt.% α-MnO_2, 0.3 wt.% α-MnO_2, and 0.5 wt.% α-MnO_2 loading in the epoxy occurred at 176.73°C, 307.87°C, 294.77°C, and 344.167°C, respectively. The 50% wt. loss for the epoxy, 0.1 wt.% α-MnO_2, 0.2 wt.% α-MnO_2, 0.3 wt.% α-MnO_2, and 0.5 wt.% α-MnO_2 loading in the epoxy occurred at temperatures of 395.12°C, 396.27°C, 403.14°C, 400.83°C, and 396.77°C, respectively. The residue was left at 550°C for samples of epoxy, 0.1 wt.% α-MnO_2, 0.2 wt.% α-MnO_2, 0.3 wt.% α-MnO_2, and 0.5 wt.% α-MnO_2 loading in the epoxy are 9.55%, 11.05%, 16.78%, 17.37% and 21.20%. If we added the weight of the residue of epoxy to the weight of these loadings and subtracted the values from the weight% left at 550°C, then we obtained the following values: 1.4%, 7.03%, 7.52%, and 11.27%, respectively, for samples containing 0.1 wt.% α-MnO_2, 0.2 wt.% α-MnO_2, 0.3 wt.% α-MnO_2, and 0.5 wt.% α-MnO_2 loading in the epoxy, which indicates that the percentage of the residue of the nanocomposites was better than that for epoxy. Consequently, in contrast to pure epoxy, the thermal stability of nanocomposites is greater, and the outcome shows that, in relation to the other specimens, the specimen with a 0.5 wt.% addition of α-MnO_2 would become heavily cross-linked. The table shows that the char residue at 5500C for the nanocomposite samples is higher
than that of epoxy, indicating that MnO_2 can hinder the thermo-oxidative decay of epoxy. The enhancement of nanocomposite thermal stability samples is due to the generation of the α-MnO_2 network structure, MnO_2's catalytic carbonization effect, and the physical barrier effect [15].

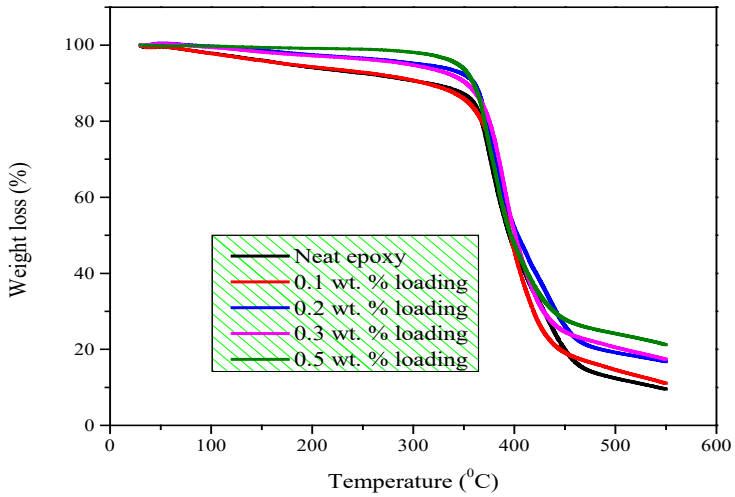

Fig. 6 TGA curves of epoxy and nanocomposite samples

Table 2 *TGA data of test samples at different temperatures*

Sample		Epoxy	0.1 wt.% loading	0.2 wt.% loading	0.3 wt.% loading	0.5 wt.% loading
Sl. no.	Temperature (°C)			% residue		
1	50	99.53	99.55	100.55	100.42	99.88
2	100	97.91	97.83	99.76	99.43	99.80
3	150	96.07	95.95	98.68	98.21	99.43
4	200	94.14	94.32	97.49	97.24	99.18
5	250	92.63	92.88	96.60	96.35	98.96
6	300	90.66	90.75	95.25	94.76	98.12
7	350	87.09	85.92	92.31	90.48	93.80
8	400	46.30	45.86	52.04	50.87	47.74
9	450	19.90	19.13	26.19	24.63	27.91
10	500	12.39	14.62	19.18	20.55	24.16
11	525	10.97	12.83	17.99	18.97	22.78
12	550	9.548	11.05	16.78	17.37	21.20

Int. Journal of Integrated Engineering Vol. 16 No. 5 (2024) p. 56-70

Table 3 *TGA data of epoxy and nanocomposites at different % of mass loss*

Sample		Epoxy	0.1 wt.% loading	0.2 wt.% loading	0.3 wt.% loading	0.5 wt.% loading
Sl. no.	% mass loss	Temperature (°C)				
1	5	175.31	176.73	307.87	294.77	344.17
2	10	314.75	312.06	360.31	352.35	359.50
3	25	372.31	375.64	376.77	380.64	374.25
4	50	395.12	396.27	403.14	400.83	396.77
5	75	438.79	428.14	453.33	447.52	484.42
6	90	541.81	-	-	-	-

3.6 Compression Test of Epoxy and Its Nanocomposites

Figure 7 presents the compressive stress-strain behavior of different wt.% loadings of α-MnO_2 for the 1st trial. The figure shows that the compressive strength of the epoxy for the 1st trial experiment is 96.62 MPa, occurring at a maximum load of 4797.69 kgf. Similarly, the compressive strengths of samples 0.1 wt.% α-MnO_2, 0.2 wt.% α-MnO_2, 0.3 wt.% α-MnO_2, and 0.5 wt.% α-MnO_2 loading for the 1st trial experiment are 59.45 MPa, 62.62 MPa, 71.87 MPa, and 73.58 MPa, corresponding to the maximum loads of 2928.54 kgf, 3059.63 kgf, 3059.63 and 3653.49 kgf, respectively. It has been seen from the figure that with the addition of reinforcement percentage of α-MnO_2 in the epoxy matrix, the compressive strength and Young's modulus of the nanocomposite decreased in comparison to epoxy. The compressive strength of 0.5 wt.% α-MnO_2 nanocomposite sample is higher compared to other nanocomposite sample due to the homogeneous dispersion of α-MnO_2 in the epoxy. The average compressive properties of epoxy and nanocomposites are presented in Table 4. The compressive stresses of samples 0.1 wt.% α-MnO_2, 0.2 wt.% α-MnO_2, 0.3 wt.% α-MnO_2, and 0.5 wt.% α-MnO_2 loading in epoxy are decreased by 38.47%, 35.1%, 25.62%, and 23.85%, respectively in comparison to the epoxy. Similarly, the compressive stress at the yield point of samples 0.1 wt.% α-MnO_2, 0.2 wt.% α-MnO_2, 0.3 wt.% α-MnO_2, and 0.5 wt.% α-MnO_2 loadings decreased by 47.27%, 37.17%, 27.98% and 28.88% respectively in comparison to the epoxy. Young's modulus of the samples 0.1 wt.% α-MnO_2, 0.2 wt.% α-MnO_2, 0.3 wt.% α-MnO_2, and 0.5 wt.% α-MnO_2 loading also decreased by 57.04%, 17.98%, 11.10%, and 36.7% respectively, as compared to epoxy. However, the compressive strain at the yield point for samples loading with 0.1 wt.%, and 0.5 wt.% are higher compared to epoxy. Generally, the α-MnO_2 reinforcing material resists stress under external force because α-MnO_2 produces more surface area to bear the load, which increases the compressive strength of the nanocomposite. However, in contrast to the epoxy, the compressive strength of the nanocomposites is low, which may be due to the shape of α-MnO_2 nanosheets, formation of pores, and agglomeration of α-MnO_2 in the epoxy matrix.

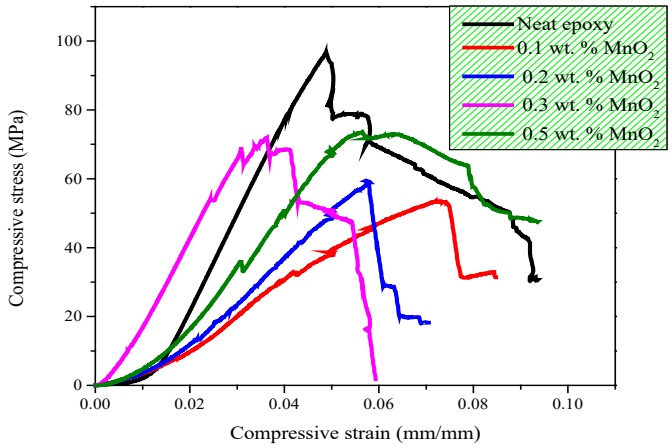

Fig. 7 *Compressive stress-strain curve of samples for trial run1*

Table 4 *Compressive characteristics of test samples*

Sl. no.	Sample	Maximum Load (kgf)	Yield Strength at Offset 0.2 % (MPa)	Compressive Strength (MPa)	Modulus (MPa)	Compressive strain (Extension) at Yield (Offset 0.2 %)
1	0.0 wt.%	4669.75	92.34	94.04	2753.18	0.047
2	0.1 wt.%	2850.44	48.68	57.86	1182.70	0.057
3	0.2 wt.%	2978.04	58.02	60.95	2258.14	0.033
4	0.3 wt.%	3417.93	66.50	69.95	2447.39	0.032
5	0.5 wt.%	3556.06	65.67	71.62	1742.73	0.055

3.7 Analysis of Compression-Fractured Surfaces

Optical microscopy was used to examine the morphologies of fractured surfaces of specimens. Figures 8(a)-8(d) show the magnification of optical microscopic (make: Curl Zeiss, model: Axiotech) images of compression fractures in samples. Figures 8(a)-8(d) show fracture surfaces of specimens with river line patterns. The smooth surface of the sample indicates that it collapsed by a brittle fracture. As a result, catastrophic propagation failures are initiated. The nanocomposite samples show the cluster formation of α-MnO_2 and micro-bubbles within the epoxy matrix. Cluster formation suggests low levels of adhesion between α-MnO_2 and epoxy. This is due to the matrix's unequal reinforcement distribution. Crack bridging is not caused by poorly scattered α-MnO2 particles, which restricts the performance of nanocomposites. These flaws serve as stress concentration areas for the production of microcracks. Because of the aggregation of α-MnO_2 inside the matrix and the creation of bubbles during the development of the nanocomposites, the compressive strength of the nanocomposites was much lower than that of pure epoxy. Pores are created in the samples as a result of the presence of air bubbles during the manufacturing process.

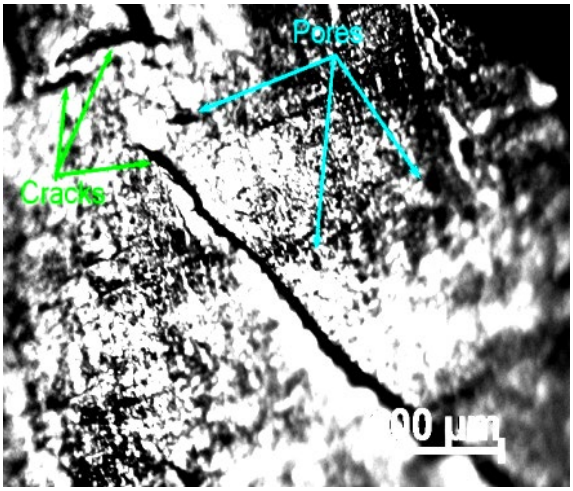

(a)

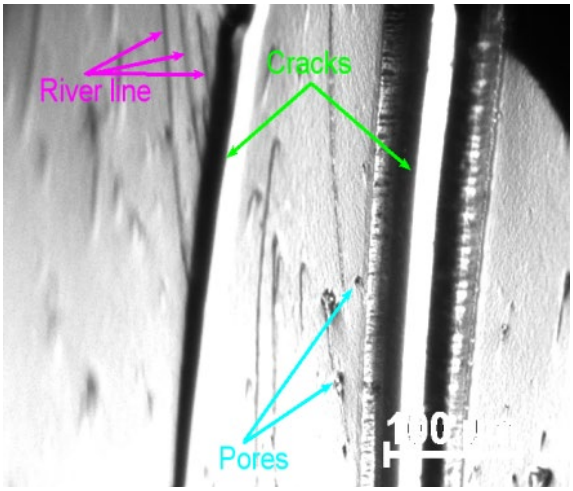

(b)

Int. Journal of Integrated Engineering Vol. 16 No. 5 (2024) p. 56-70

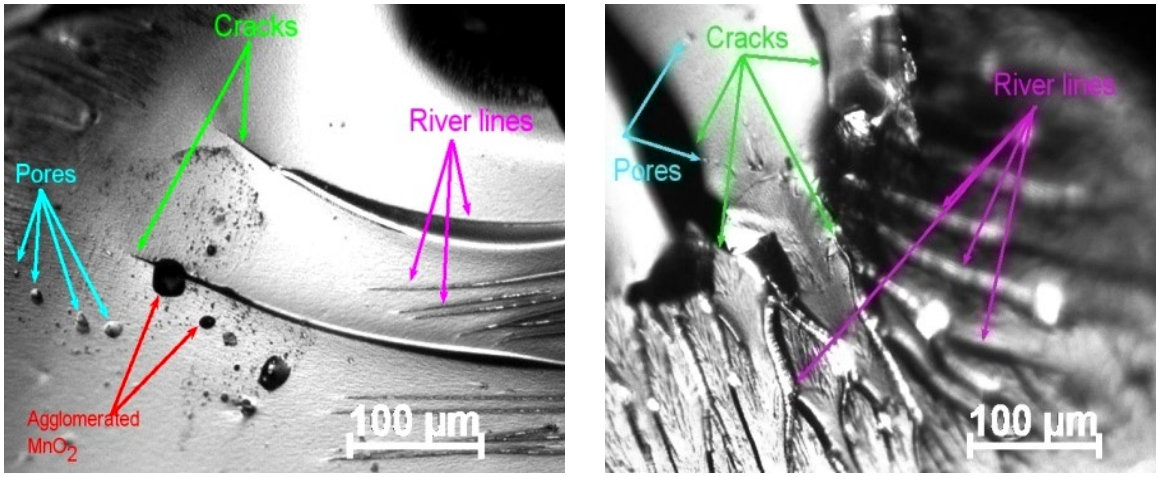

(c) **(d)**

Fig. 8 *Worn surfaces of samples (a) epoxy; (b) 0.1 wt.% loading; (c) 0.3 wt.% loading; (d) 0.5 wt.% loading; loading of α-MnO_2*

The HRFESEM images of the fractured surfaces of test samples are shown in Figures 9(a)-9(d). All of the fractured pathways in these images are river line patterns, suggesting brittle collapse. Figure 9(a) illustrates fine cracks induced by brittle fractures in pristine epoxy. The cracks become less randomly distributed, as shown in Figures 9(b)-9(d) with the addition of α-MnO_2, indicating that the α-MnO_2 network did not act as an impediment to crack propagation and was unable to cause the crack path to deviate [44]. As a result, the bonding between α-MnO2 in epoxy can reduce the strength of epoxy nanocomposites. Figure 7 shows that the epoxy samples have high compressive strength. This is due to the rough surface and many random cracks. This may be because the epoxy limits crack propagation, and microcracks form in the stress concentration zone with increasing stress. These microcracks unite to form a characteristic crack pattern on the surface of the epoxy matrix. This is known as a crack pattern or crack cluster [45]. Nassar & Nassar established that the tensile behavior and elastic modulus of epoxies reinforced with SiC nanoparticles decreased with increasing reinforcement amounts. This is attributed to the strong cooperation between the materials. Wear data showed that the wear behavior of unreinforced epoxy was elevated with the addition of SiC particles. So that the counter surface on which the ceramic nanoparticles migrate did not look like a smooth surface [46]. The compressive strength of nanocomposites is less than that of epoxy, which may be due to the existence of agglomerated α-MnO_2, the shape of α-MnO_2, and the formation of more micro-voids during the fabrication process [46-50]. The α-MnO_2 nanosheets act as stress-raisers, which can reduce the compressive strength of the epoxy. Therefore, the reinforced α-MnO_2 nanosheets in the epoxy matrix did not play a serious role in improving the compressive strength of the nanocomposites.

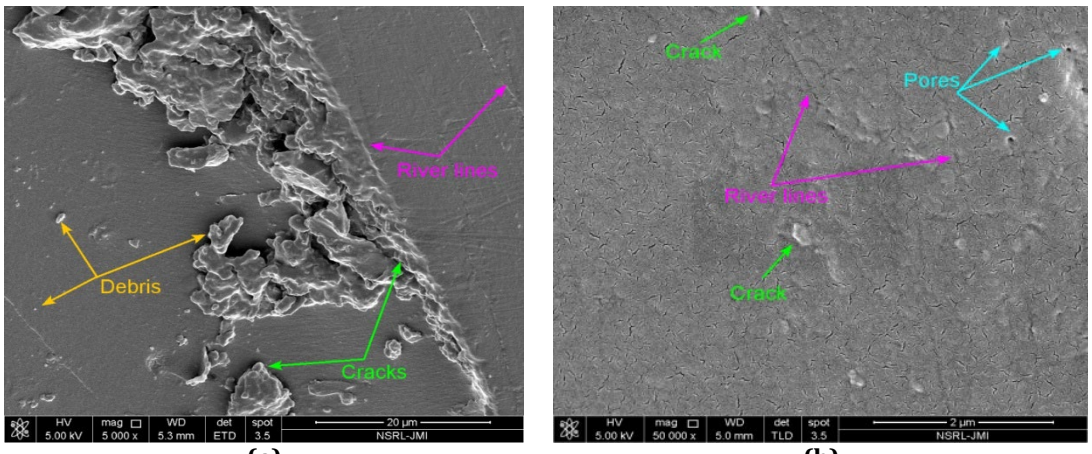

(a) **(b)**

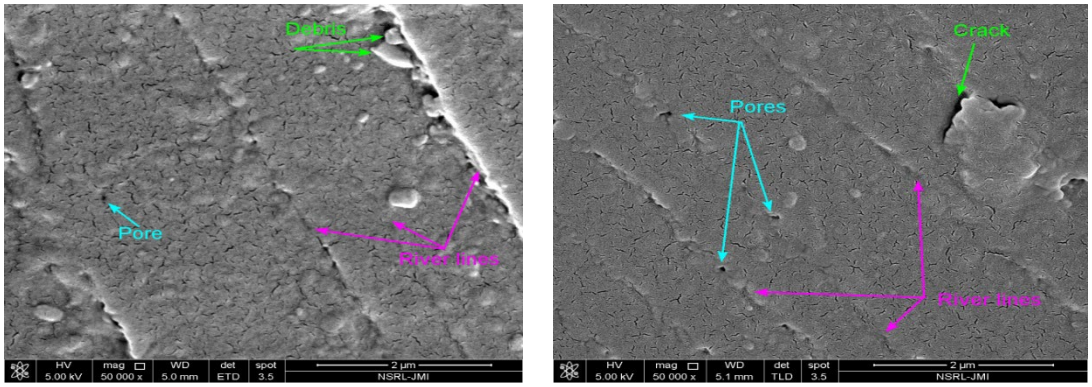

(c) (d)

Fig. 9 *Worn surfaces of samples (a) epoxy; (b) 0.1 wt.%; (c) 0.3 wt.%; (d) 0.5 wt.% loading of α-MnO_2 at x50,000 during compression test*

Figures 10(a)-10(b) show HRFESEM images of the nanocomposite samples. The figures show agglomerated particles on the surface of nanocomposites. The abrupt decrease in compressive strength values with α-MnO_2 loading may be attributed to molecule agglomeration in the epoxy, as these agglomerates tend to block the reactive sites present in the nano-α-MnO_2. As the agglomerated molecules grow in size, there are fewer reactive sites left in the nanofiller. As a result, the reduced compressive properties of the nanocomposite samples compared to the pure epoxy could be associated to void creation and low dispersion of α-MnO_2 in the epoxy.

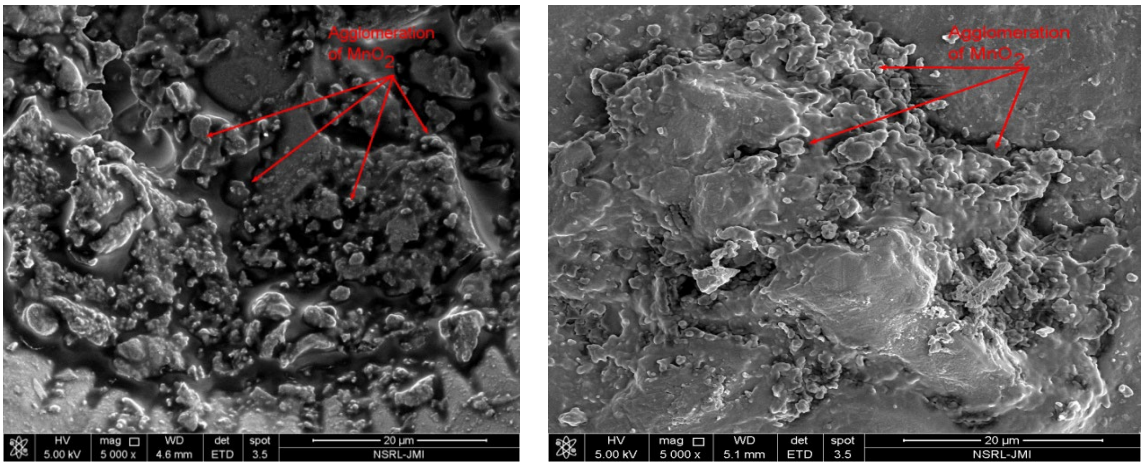

(a) (b)

Fig. 10 *Neat images of samples (a) 0.1 wt.%; (b) 0.2 wt.% loading of α-MnO_2*

4. Conclusion

A thorough analysis of the results allows us to draw the following conclusions:

(i) A solution approach was used to create α-MnO_2/epoxy nanocomposites successfully.

(ii) The formation of α-MnO_2 nanosheets was verified by X-ray diffraction, high-resolution scanning electron microscopy pictures, and energy-dispersive X-ray analyses.

(iii) The density of the nanocomposites increases with an increase in the wt.% loading of α-MnO_2 owing to the existence of high-density α-MnO_2 in the epoxy.

(iv) Increasing the amount of α-MnO_2 inclusion increased the glass transition temperature of the epoxy. The TGA results show that the % residue of the nanocomposite was larger than that of the epoxy. Since the thermal stability of nanocomposites is higher than that of pure epoxy, the samples with 0.5 wt.% α-MnO_2 are cross-linked to a greater extent than the other samples.

(v) Due to the inclusion of α-MnO_2 in the epoxy, the compressive stress of samples 0.1 wt.%, 0.2 wt.%, 0.3 wt.%, and 0.5 wt.% loading of α-MnO_2 are decreased by 38.47%, 35.1%, 25.62%, and 23.85% respectively, in contrast to the epoxy. The compressive strength of the developed nanocomposites is lower in contrast to epoxy, which may be by virtue of pore formation, aggregation of α-MnO_2 within the epoxy matrix, and the shape of the reinforcement.

(vi) Microscopic images revealed the formation of air voids amid the manufacture of the nanocomposites and the aggregation of α-MnO_2 within the matrix. This significantly reduced the compressive properties of nanocomposites.

Therefore, we can conclude that the α-MnO_2/epoxy nanocomposite can be widely utilized as a thermally heat-resistant material in the future.

Acknowledgment

The authors appreciate the feedback and suggestions of Dr. Sabah Khan, Professor, Department of Mechanical Engineering, Jamia Millia Islamia, Jamia Nagar, New Delhi, India.

Conflicts of Interest

The authors have declared that there are no conflicts of interest.

Author Contribution

The authors confirm their contributions to the work as follows: ***Conceptualization****, Md. Zakir Hussain;* ***methodology****, Md. Zakir Hussain and Pranjal Sarmah;* ***analysis and interpretation of results****, Md. Zakir Hussain and Pranjal Sarmah;* ***resources****, Pranjal Sarmah;* ***writing—original draft preparation****, Md. Zakir Hussain and Pranjal Sarmah;* ***writing—review and editing****, Md. Zakir Hussain and Pranjal Sarmah;* ***visualization****, Md. Zakir Hussain;* ***supervision****, Pranjal Sarmah. After reviewing the findings, all authors gave their approval to the final version of the manuscript.*

References

[1] Król-Morkisz, K. & Pielichowska, K. (2019). Thermal Decomposition of Polymer Nanocomposites With Functionalized Nanoparticles. In K. Pielichowski & T.M. Majka (Eds.), *Polymer Composites with Functionalized Nanoparticles: Synthesis, Properties, and Applications* (pp. 405–435). Elsevier: Kraków, Poland. https://doi.org/10.1016/B978-0-12-814064-2.00013-5

[2] Ajayan, P. M., Schadler, L. S., & Braun, P. V. (2003). *Nanocomposite science and technology*. WileyVCHVerlag GmbH, Weinheim.

[3] Tjong, S.C. (2006). Structural and mechanical properties of polymer nanocomposites. *Materials Science and Engineering: R: Reports*. 53(3-4), 73-197. https://doi.org/10.1016/j.mser.2006.06.001

[4] Park, C. I., Park, O. O., Lim, J. G., & Kim, H. J. (2001). The fabrication of syndiotactic polystyrene/organophilic clay nanocomposites and their properties. *Polymer*, 42(17), 7465-7475. https://doi.org/10.1016/S0032-3861(01)00213-0

[5] Khan, A., Aziz, T., Shah, S.S.A., Rauf, A., Zubair, Z., Shah, S.A.A., Saeedullah, S., Sulaiman, S., & Thebo, K.H. (2016). Functionalized Multi-Walled Carbon Nanotube-Reinforced Epoxy-Composites: Electrical And Mechanical Characterization. *International Journal of Advanced Engineering, Management and Science*, 2(12), 1970-1976.

[6] Biron, M. (2003). Thermosets and composites, Elsevier.

[7] Abdellaoui, H., Raji, M., & Bouhfid, R. (2019). Investigation of the deformation behavior of epoxy-based composite materials. In M. Jawaid, M. Thariq, & N. Saba (Eds.), *Failure analysis in biocomposites, fibre-reinforced composites and hybrid composites*, Amsterdam: Elsevier, 29-49. https://doi.org/10.1016/B978-0-08-102293-1.00002-4

[8] Xia, H., Feng, J., Wang, H., Lai, M. O., & Lu, L. (2010). MnO_2 nanotube and nanowire arrays by electrochemical deposition for supercapacitor. *Journal of Power Sources*, 195(13), 4410-4413. https://doi.org/10.1016/j.jpowsour.2010.01.075

[9] Xu, C., Zhao, Y., Yang, G., Li, F., & Li, H. (2009). Mesoporous nanowire array architecture of manganese dioxide for electrochemical capacitor applications. *Chemical Communications*, (48), 7575-7577. https://doi.org/10.1039/B915016A

[10] Ma, R. E., Bando, Y., Zhang, L. I., & Sasaki, T. (2004). Layered MnO_2 nanobelts: hydrothermal synthesis and electrochemical measurements. *Advanced Materials*, 16(11), 918-922. https://doi.org/10.1002/adma.200306592

[11] Yang, Z., Zhang, Y., Zhang, W., Wang, X., Qian, Y., Wen, X., & Yang, S. (2006). Nanorods of manganese oxides: synthesis, characterization and catalytic application. *Journal of Solid State Chemistry*, 179(3), 679-684. https://doi.org/10.1016/j.jssc.2005.11.028

[12] Zhang, W., Yang, Z., Wang, X., Zhang, Y., Wen, X., & Yang, S. (2006). Large-scale synthesis of β-MnO_2 nanorods and their rapid and efficient catalytic oxidation of methylene blue dye. *Catalysis Communications*, 7(6), 408-412. https://doi.org/10.1016/j.catcom.2005.12.008

[13] Balguri, P. K., Thumu, UD. G, H.S.; Penki, T.R., & Chilumala, I. (2022). Manganese dioxide nanostructures reinforced epoxy nanocomposites: a study of mechanical properties. *Polymer-Plastics Technology and Materials*, 61(4), 441-460. https://doi:10.1080/25740881.2021.1991953
[14] Hussain, M. Z., & Khan, S. (2022). Fabrication and tribological behavior of MnO2/epoxy nanocomposites. *High Performance Polymers*, 34(7), 742–758. https://doi.org/10.1177/09540083221079
[15] Qian, X., Shi, C., & Jing, J. (2020). CNT modified layered α-MnO_2 hybrid flame retardants: preparation and their performance in the flame retardancy of epoxy resins. *RSC Advances*, 10(46), 27408-27417. https://doi.org/10.1039/D0RA03654D
[16] Zhou, Y., Li, L., Chen, Y., Zou, H., & Liang, M. (2015). Enhanced mechanical properties of epoxy nanocomposites based on graphite oxide with amine-rich surface. *RSC Advances*, 5(119), 98472-98481. https://doi.org/10.1039/C5RA22458F
[17] Che Nasir, N. A., Saharudin, M. S., Wan Jusoh, W. N., & Kooi, O. S. (2022). Effect of Nanofillers on the Mechanical Properties of Epoxy Nanocomposites. In A. Ismail, W.M. Dahalan, & A. Öchsner (Eds.) *Design in Maritime Engineering, Advanced Structured Materials*. vol.167 Springer, Cham. https://doi.org/10.1007/978-3-030-89988-2_15.
[18] Lee, D., Song, S. H., Hwang, J., Jin, S.H., Park, K. H., Kim, B. H., Hong, S. H., & Jeon, S. (2013). Enhanced mechanical properties of epoxy nanocomposites by mixing noncovalently functionalized boron nitride nanoflakes. *Small*, 9(15), 2602-2610. https://doi.org/10.1002/smll.201203214
[19] Kesavulu, A., & Mohanty, A. (2022). Investigation of physical, flexural, and dynamic mechanical properties of alumina and graphene nanoplatelets filled epoxy nanocomposites. *Polymer Composites*, 43(5), 2711-2723. https://doi.org/10.1002/pc.26568
[20] Wu, Y., Tang, B., Liu, K., Zeng, X., Lu, J., Zhang, T., & Shen, X. (2019). Enhanced flexural properties of aramid fiber/epoxy composites by graphene oxide. *Nanotechnology Reviews*, 8(1), 484-492. https://doi.org/10.1515/ntrev-2019-0043
[21] Yusuf, S., Islam, N., Akram, W., Ali, H., & Siddique, A. (2020). Prediction of the best tensile and flexural strength of natural fiber reinforced epoxy resin-based composite using taguchi method. Proceedings of the International Conference on Industrial & Mechanical Engineering and Operations Management, 26-27 December, Dhaka, Bangladesh.
[22] Reddy, S. P., Rao, P. C., Reddy, A. C., & Parmeswari, G. (2014). Tensile and flexural strength of glass fiber epoxy composites. In International Conference on Advanced Materials and manufacturing Technologies (AMMT 2014), 18 December, Paramount Publishing House, Hyderabad, India, 98-102.
[23] Hamim, S.U., & Singh, R. P. The effect of clay on the mechanical properties of epoxy resins subjected to hygrothermal ageing. Retrieved December 12, 2022, from https://doi.org/10.48550/arXiv.1611.05144.
[24] Khan, S., Bari, P., & Mishra, S. (2019). Effect of chemically reduced graphene oxide on mechanical and thermal properties of epoxy nano composites. *Journal of Materials Science & Nanotechnology*, 7(2), 1-9.
[25] Norhakim, N., Ahmad, S. H., Chia, C. H., & Huang, N. M. (2014). Mechanical and thermal properties of graphene oxide filled epoxy nanocomposites. *Sains Malaysian*, 43(4), 603-609.
[26] Mohammed, S. M., Khalil, T. A., Mahmoud, T. S., & El-Kady, E. Y. (2016). Effect of Al_2O_3 and mwcnts nanofillers on the mechanical characteristics of epoxy-based polymeric matrix nanocomposites. *Nano Science & Nano Technology: An Indian Journal*, 10(2); 41-50.
[27] Ergün, YA. (2019). Mechanical Properties of Epoxy Composite Materials Produced with Different Ceramic Powders. *Journal of Materials Science and Chemical Engineering*, 7(12), 1-8. https://doi.org/10.4236/msce.2019.712001.
[28] Ávila, A. F., Peixoto, L. D., Silva Neto, A., Ávila Junior, J. D., & Carvalho, M. G. (2012). Bending investigation on carbon fiber/epoxy composites nano-modified by grapheme. Journal of the *Brazilian Society of Mechanical Sciences and Engineering*. 34(3), 269-275. https://doi.org/10.1590/S1678-58782012000300007
[29] Siegfried, M., Tola, C., Claes, M., Lomov, S.V., Verpoest, I., & Gorbatikh, L. (2014). Impact and residual after impact properties of carbon fiber/epoxy composites modified with carbon nanotubes. *Composite Structures*, 111, 488-496. https://doi.org/10.1016/j.compstruct.2014.01.035
[30] Singh, S., Srivastava, V. K., & Prakash, R. (2013). Characterisation of multi-walled carbon nanotube reinforced epoxy resin composites. *Materials Science and Technology*, 29(9), 1130-1134. https://doi.org/10.1179/1743284713Y.0000000288
[31] Srivastava, V. K., & Singh, S. (2012). A micro-mechanical model for elastic modulus of multi-walled carbon nanotube/epoxy resin composites. *International Journal of Composite Materials*, 2(2), 1-6. https://doi.org/10.5923/j.cmaterials.20120202.01
[32] Giovannelli, A., Di Maio, D., & Scarpa, F. (2017). Industrial-graded epoxy nanocomposites with mechanically dispersed multi-walled carbon nanotubes, static and damping properties. *Materials*, 10(10), 1222. https://doi.org/10.3390/ma10101222
[33] RTO Lecture Series, Nanotechnology aerospace applications. EN-AVT-129, 2005.

[34] Wang, W., Pan, Y., Pan, H., Yang, W., Liew, K.M., Song, L., & Hu, Y. (2016). Synthesis and characterization of MnO2 nanosheets based multilayer coating and applications as a flame retardant for flexible polyurethane foam. *Composites Science and Technology*, 123, 212-221. https://doi.org/10.1016/j.compscitech.2015.12.014
[35] Wang, W, Kan, Y., Yu, B., Pan, Y., Liew, K. M., Song, L., & Hu, Y. (2017). Synthesis of MnO_2 nanoparticles with different morphologies and application for improving the fire safety of epoxy. *Composites Part A: Applied Science and Manufacturing*, 95, 173-182. https://doi.org/10.1016/j.compositesa.2017.01.009
[36] Xu, D., Li, B., Wei, C., He, Y. B., Du, H., Chu, X., Qin, X., Yang, Q. H., & Kang, F. (2014). Preparation and characterization of MnO2/acid-treated CNT nanocomposites for energy storage with zinc ions. *Electrochimica Acta*, 133, 254-261. https://doi.org/10.1016/j.electacta.2014.04.001
[37] Hussain, M. Z., Khan, S., Nagarajan, R., Khan, U., & Vats, V. (2016). Fabrication and microhardness analysis of MWCNT/MnO_2 nanocomposite, *Journal of Materials*, 2016, 6070468. http://dx.doi.org/10.1155/2016/6070468
[38] Sannasi, V., & Subbian, K. (2020). Influence of Moringa oleifera gum on two polymorphs synthesis of MnO_2 and evaluation of the pseudo-capacitance activity. *Journal of Materials Science: Materials in Electronics*, 31(19), 17120-17132. https://doi.org/10.1007/s10854-020-04272-z
[39] Hlaing, A. A., & Win, P. P. (2012). The synthesis of α-MnO_2 nanorods using hydrothermal homogeneous precipitation. *Advances in Natural Sciences: Nanoscience and Nanotechnology*, 3(2), 025001. https://doi.org/10.1088/2043-6262/3/2/025001
[40] Hussain, M., Khan, S., Sarmah, P., & Khan, U. (2018). Analysis of erosive wear of MWCNTs/MnO_2 nanocomposite. *Materials Today: Proceedings*, 5(11), 23559-23567. https://doi.org/10.1016/j.matpr.2018.10.144
[41] Shah, S.I., Khan, T., Khan, R., Khan, S.A., Khattak, S.A., & Khan, G. (2019). Study of structural, optical and dielectric properties of α-MnO_2 nanotubes (NTS). *Journal of Materials Science: Materials in Electronics*, 30 (21), 19199-19205. https://doi.org/10.1007/s10854-019-02277-x
[42] Zou, M. M., & Ai, D. J., & Liu, K. Y. (2011). Template synthesis of MnO_2/CNT nanocomposite and its application in rechargeable lithium batteries. *Transactions of Nonferrous Metals Society of China*, 21(9), 2010-2014. https://doi.org/10.1016/S1003-6326(11)60964-3
[43] Chen, B., Chen, J., Li, J. Y., Tong, X., Zhao, H. C., & Wang, L. P. (2017). Oligoaniline assisted dispersion of carbon nanotubes in epoxy matrix for achieving the nanocomposites with enhanced mechanical, thermal and tribological properties. *Chinese Journal of Polymer Science*, 35 (3), 446-454. https://doi.org/10.1007/s10118-017-1911-z
[44] Zhang, M., Zhai, Z., Li, M., Cheng, T., Wang, C., Jiang, D., Chen, L., Wu, Z., & Guo, Z. (2016). Epoxy nanocomposites with carbon nanotubes and montmorillonite: Mechanical properties and electrical insulation. *Journal of Composite Materials*, 50(24), 3363-3372. https://doi.org/10.1177/0021998315620000
[45] Szeląg, M. (2019). Properties of cracking patterns of multi-walled carbon nanotube-reinforced cement matrix. *Materials*, 12(18), 2942. https://doi.org/10.3390/ma12182942
[46] Nassar, A., & Nassar, E. (2013). Study on mechanical properties of epoxy polymer reinforced with Nano-SiC particles. *Nanoscience and nanoengineering*, 1(2), 89-93. https://doi.org/10.13189/nn.2013.010201
[47] Ervina, J., Mariatti, M., & Hamdan, S. (2016). Effect of filler loading on the tensile properties of multi-walled carbon nanotube and graphene nanopowder filled epoxy composites. *Procedia Chemistry*, 19, 897-905. https://doi.org/10.1016/j.proche.2016.03.132
[48] Wei, J., Vo, T., & Inam, F. (2015). Epoxy/graphene nanocomposites–processing and properties: a review. *RSC Advances*, 5 (90), 73510-73524. https://doi.org/10.1039/C5RA13897C
[49] Choi, Y. M., Hwangbo, S., Lee, T. G., & Ham, Y. B. (2021). Effect of particle size on the mechanical properties of TiO2-epoxy nanocomposites. *Materials*, 14(11), 2866. https://doi.org/10.3390/ma14112866
[50] Suriati, G., Mariatti, M., & Azizan, A. (2011). Effects of filler shape and size on the properties of silver filled epoxy composite for electronic applications. *Journal of Materials Science: Materials in Electronics*. 22(1), 56-63. https://doi.org/10.1007/s10854-010-0082-2